Thomas, G. A., & Peticolas, W. L. (1983a) *J. Am. Chem. Soc. 105*, 986–992.
Thomas, G. A., & Peticolas, W. L. (1983b) *J. Am. Chem. Soc. 105*, 993–996.
Thomas, G. J., Jr., & Hartman, K. A. (1973) *Biochim. Biophys. Acta 312*, 311.
Viswamitra, M. A., Kennard, O., Shakked, Z., Jones, P. G., Sheldrick, B. M., Salisburg, S., & Pauello, L. (1978) *Nature (London) 273*, 687–690.
Wang, A. H. J., Quigley, G. J., Kolpak, F. J., Crawford, J. L., van Boom, J. H., van der Marel, G., & Rich, A. (1979) *Nature (London) 282*, 680–686.
Wang, A. H. J., Quigley, G. J., Kolpak, F. J., van der Marel, G., van Boom, J. H., & Rich, A. (1981) *Science (Washington, D.C.) 211*, 171–176.
Wing, R., Drew, H., Takano, T., Broka, C., Tanaka, S., Itakura, K., & Dickerson, R. E. (1980) *Nature (London) 287*, 755–758.

Deoxyguanosine–Deoxyadenosine Pairing in the d(C-G-A-G-A-A-T-T-C-G-C-G) Duplex: Conformation and Dynamics at and Adjacent to the dG·dA Mismatch Site†

Dinshaw J. Patel,* Sharon A. Kozlowski, Satoshi Ikuta, and Keiichi Itakura

ABSTRACT: Nuclear magnetic resonance (NMR) has been used to monitor the conformation and dynamics of the d-(C_1-G_2-A_3-G_4-A_5-A_6-T_6-T_5-C_4-G_3-C_2-G_1) self-complementary dodecanucleotide (henceforth called 12-mer GA) that contains a dG·dA purine–purine mismatch at position 3 in the sequence. These results are compared with the corresponding d(C-G-C-G-A-A-T-T-C-G-C-G) dodecamer duplex (henceforth called 12-mer) containing standard Watson–Crick base pairs at position 3 [Patel, D. J., Kozlowski, S. A., Marky, L. A., Broka, C., Rice, J. A., Itakura, K., & Breslauer, K. J. (1982) *Biochemistry 21*, 428–436]. The dG·dA interaction at position 3 was monitored at the guanosine exchangeable H-1 and nonexchangeable H-8 protons and the nonexchangeable adenosine H-2 proton. We demonstrate base-pair formation between anti orientations of the guanosine and adenosine rings on the basis of nuclear Overhauser effects (NOE) observed between the H-2 proton of adenosine 3 and the imino protons of guanosine 3 (intra base pair) and guanosines 2 and 4 (inter base pair). The dG(anti)·dA(anti) pairing should result in hydrogen-bond formation between the guanosine imino H-1 and carbonyl O-6 groups and the adenosine N-1 and NH_2-6 groups, respectively. The base pairing on either side of the dG·dA pair remains intact at low temperature, but these dG·dC pairs at positions 2 and 4 are kinetically destabilized in the 12-mer GA compared to the 12-mer duplex. We have estimated the hydrogen exchange kinetics at positions 4–6 from saturation-recovery measurements on the imino protons of the 12-mer GA duplex between 5 and 40 °C. The measured activation energies for imino proton exchange in the 12-mer GA are larger by a factor of ~2 compared to the corresponding values in the 12-mer duplex. This implies that hydrogen exchange in the 12-mer GA duplex results from a cooperative transition involving exchange of several base pairs as was previously reported for the 12-mer containing a G·T wobble pair at position 3 [Pardi, A., Morden, K. M., Patel, D. J., & Tinoco, I., Jr. (1982) *Biochemistry 21*, 6567–6574]. We have assigned the nonexchangeable base protons by intra and inter base pair NOE experiments and monitored these assigned markers through the 12-mer GA duplex to strand transition. We demonstrate that replacing two dG·dC by two dG·dA base pairs reduces the melting temperature of the dodecanucleotide by ~17 °C. The phosphorus spectrum of the 12-mer GA differs significantly from that of the 12-mer, indicative of changes in the phosphodiester backbone in order to accommodate the dG(anti)·dA(anti) base-pair formation in the interior of a DNA duplex.

There has been a great deal of recent experimental (Neidle & Berman, 1983; Patel et al., 1982a) and theoretical (Olson, 1982; Tilton et al., 1983; Olson et al., 1983; Levitt, 1983; Tidor et al., 1983) activity aimed at elucidating the conformational features of DNA in the crystalline (Dickerson et al., 1983; Viswamitra, 1983; Wang et al., 1983), fiber (Arnott et al., 1983; Zimmerman & Pfeiffer, 1983), and solution (Pardi et al., 1981; Patel et al., 1983a; Feigon et al., 1983) states. Much less is known about the role of non-Watson–Crick pairing and the consequences base-pair mismatches at and adjacent to the modification site. (Lomant & Fresco, 1975; Topal & Fresco, 1976a,b; Rein et al., 1983; Haasnoot et al., 1979, 1980; Wallace et al., 1979).

The most definitive investigations have focused on the G·U interaction in transfer RNA (Schimmel & Redfield, 1980; Hare & Reid, 1982) and the dG·dT interaction in DNA duplexes (Early et al., 1978; Patel et al., 1982c). This purine–pyrimidine mismatch involves two imino proton–carbonyl group hydrogen bonds on the basis of a nuclear Overhauser effect (NOE) between the guanosine and thymidine protons in the wobble pair.

There are few reports on purine–purine mismatches in nucleic acid duplexes. One example has been observed for yeast phenylalanine transfer RNA crystals, which contain a

†From AT&T Bell Laboratories, Inc., Murray Hill, New Jersey 07974 (D.J.P. and S.A.K.), and the Molecular Genetics Department, City of Hope National Medical Center, Duarte, California 91010 (S.I. and K.I.). *Received November 7, 1983.* The high-field NMR experiments were performed at the NMR facility for biomedial research located at the Francis Bitter National Magnet Laboratory, Massachusetts Institute of Technology. The NMR facility is supported by Grant RR0095 from the Division of Research Resources (National Institutes of Health) and by the National Science Foundation under Contract C-670. The contributions of S.I. and K.I. were funded by NIH Grant GM 28651.

0006-2960/84/0423-3207$01.50/0

Chart I

C	G	C	G	A	A	T	T	C	G	C	G
1	2	3	4	5	6	6	5	4	3	2	1
G	C	G	C	T	T	A	A	G	C	G	C

Chart II

C	G	A	G	A	A	T	T	C	G	C	G
1	2	3	4	5	6	6	5	4	3	2	1
G	C	G	C	T	T	A	A	G	A	G	C

m_2^2G(26)·A(44) pairing at the end of a helical stem (Kim, 1981). The single-crystal X-ray studies demonstrate that both bases are anti and that the pairing is stabilized by two Watson–Crick hydrogen bonds. Alternate models with one of the purines in the syn configuration resulting in two Hoogsteen hydrogen bonds have also been put forward for the G·A interaction in ribosomal RNA duplexes (Traub & Sussman, 1982).

Thermal melting investigations by Dodgson & Wells (1977a,b) have demonstrated that dG·dA mismatches destabilize the duplex but do not disrupt the cooperative interaction between flanking dG·dC base pair segments in $(dG)_n$·$(dC_{12}A_mC_x)$ duplexes where $m = 1$–6. They further demonstrated that single dG·dA mismatches were extremely resistant to S1 and mung bean single strand specific nucleases with the nuclease sensitivity increasing as the length of adjacent dG·dA mismatches increased from 1 to 6 (Dodgson & Wells, 1977a,b).

The d(C-G-C-G-A-A-T-T-C-G-C-G) self-complementary dodecanucleotide duplex (henceforth called 12-mer; Chart I) has been extensively investigated by single-crystal X-ray (Dickerson et al., 1982, 1983) and solution NMR investigations (Patel et al., 1982b; Pardi et al., 1982; Hare et al., 1983). We have begun a systematic investigation of the consequences of replacing the Watson–Crick dC·dG base pair by dT·dG, dA·dG, dC·dA, and dC·dT pairs at position 3 in the 12-mer duplex. We have previously reported on a detailed NMR and calorimetric investigation of 12-mer GT duplex (Patel et al., 1982c,d) and report below on an NMR investigation of the d(C-G-A-G-A-A-T-T-C-G-C-G) self-complementary dodecanucleotide duplex (henceforth called 12-mer GA; Chart II), which contains two symmetry-related dG·dA interactions.

The marked improvement in spectral resolution at high fields and the introduction of NOE methods to establish rigorous NMR spectral assignments have provided resolved and assigned proton markers at the individual base-pair level in DNA duplexes (Patel et al., 1982a, 1983a; Kan et al., 1982; Pardi et al., 1981; Early et al., 1980; Feigon et al., 1983; Hare et al., 1983; Kaptein et al., 1983; Weiss et al., 1984; Reid et al., 1983). Thus, it is possible to characterize conformational and dynamic features at and adjacent to the mismatch site in oligonucleotide duplexes.

Experimental Procedures

NMR Spectroscopy. Proton spectra were recorded on a 498-MHz NMR spectrometer at the Francis Bitter National Magnet Laboratory, MIT, and on a Varian XL-200 spectrometer. Proton spectra in H_2O were accumulated with a Refield 214 or a time-shared long-pulse method (Redfield et al., 1981). The nuclear Overhauser effect and saturation recovery data involving a set of decoupling frequencies or time delays were accumulated in the interleave mode. The experimental conditions are included in the figure captions. Phosphorus spectra were accumulated on a Varian XL-200 spectrometer. Chemical shifts are corrected for the temperature dependence of the internal standard trimethyl phosphate.

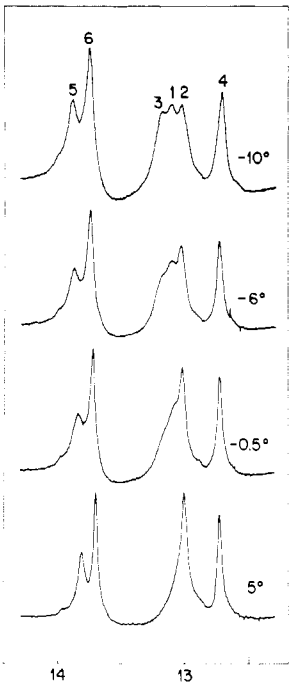

FIGURE 1: The 498-MHz proton NMR spectra of the 12-mer GA duplex in 0.1 M NaCl, 5 mM phosphate, 1 mM ethylenediaminetetracetic acid (EDTA), and 4:1 H_2O–D_2O, pH 6.75, as a function of temperature between −10 and 5 °C.

Synthesis. The 12-mer GA sequence was synthesized in milligram amounts by the solid-phase triester method reported previously (Tan et al., 1983). The procedure consists of attaching the 3′-terminal nucleoside of the desired sequence to the polystyrene copolymer support through a 1% divinylbenzene linkage. The mononucleotide or dinucleotide coupling units were sequentially added through their 3′ ends to the growing nucleotide chain on the insoluble support until the desired sequence was built. The dimer couplings to yield the 12-mer GA sequence were undertaken with percentage yields of 90, 92, 88, 90, and 92, respectively, on proceeding from the 3′ to the 5′ end. The final product was cleaved from the solid support, the protecting groups were deblocked, and the 12-mer GA was purified on DEAE-cellulose DE-52 followed by size-exclusion chromatography on G-75 or G-50. This procedure yielded 160 A_{260} units of the 12-mer GA sequence. The high-temperature proton NMR spectrum of the 12-mer GA confirmed the purity of the dodecanucleotide.

Concentration. The proton NMR spectra were recorded on 80 A_{260} units of 12-mer GA in 0.2 mL of 0.1 M phosphate buffer. The samples were diluted by a factor of 2 to record the phosphorus NMR spectra.

Results

Imino Proton Spectra in 5 mM Phosphate. We have recorded the imino proton spectra of the 12-mer GA in 0.1 M NaCl–5 mM phosphate buffer, pH 6.75, as a function of temperature with spectra between −10 and 5 °C shown in Figure 1. The low phosphate buffer concentration and pH values below neutrality were used since phosphate and base both catalyze hydrogen exchange of protons toward the end of the duplex (Patel & Hilbers, 1975; Fritzsche et al., 1983). We observe six resonances in the imino proton spectra at −10

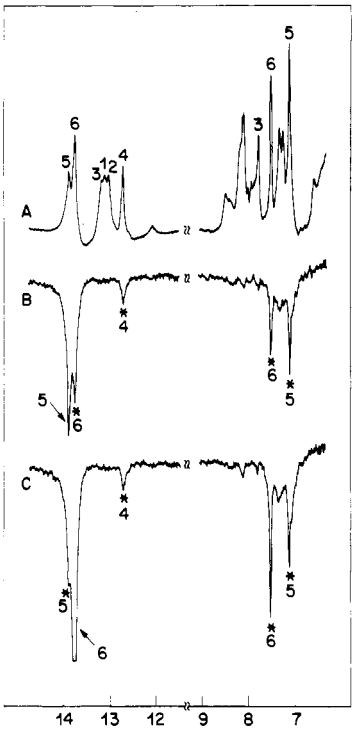

FIGURE 2: (A) The 498-MHz proton NMR spectra (11.5–14.5 ppm; 6.5–9.0 ppm) of the 12-mer GA duplex in 0.1 M NaCl, 5 mM phosphate, 1 mM EDTA, and 4:1 H_2O–D_2O, pH 6.75, at −10 °C. Difference spectra following 1-s saturation of (B) the 13.90 ppm thymidine imino proton and (C) the 13.77 ppm thymidine imino proton. Saturation power levels resulted in ~50% saturation of the desired resonance. The saturated resonance is designated by an arrow while the observed NOEs are designated by asterisks.

°C with the resonances at 13.20 and 13.13 ppm broadening out in a sequential manner on raising the temperature to 5 °C (Figure 1) and the resonance at 13.05 ppm broadening out at 25 °C.

NOEs between Imino Protons. We have recorded the NOE between imino protons on adjacent base pairs in the 12-mer GA duplex in 0.1 M NaCl–5 mM phosphate, pH 6.75, at −10 and 5 °C. The predominant interactions are between adjacent base pairs at 5 °C with spin diffusion becoming more important at −10 °C.

We observe six resonances for the imino protons of the 12-mer GA at −10 °C with the two resonances to low field of 13.5 ppm assigned to the dA·dT thymidine imino protons while the four resonances to high field 13.5 ppm assigned to the dG·dC and dG·dA guanosine imino protons (Figure 2A). An NOE is observed at the 12.74 ppm guanosine imino proton on saturation of the partially resolved thymidine imino protons at 13.90 (Figure 2B) and 13.77 ppm (Figure 2C) in the 12-mer GA spectrum at −10 °C. This effect persists on saturation of the 13.90 ppm resonance but to a lesser extent on saturation of the 13.77 ppm resonance in difference spectra recorded at 5 °C (not shown). These observations permit assignment of the 13.90 ppm resonance to the thymidine imino proton of base pair 5, the 13.77 ppm resonance to the thymidine imino proton of base pair 6, and the 12.74 ppm resonance to the guanosine imino proton of base pair 4 in the 12-mer GA sequence (Table I).

We observe an inter base pair NOE at the 12.74 ppm imino proton of dG·dC base pair 4 on saturation of the 13.20 ppm imino proton (Figure 3B), permitting assignment of this resonance to the imino proton of the dG·dA interaction at position 3 in the sequence (Table I). The guanosine imino proton at 13.13 ppm broadens before the one at 13.05 ppm on raising the temperature of the 12-mer GA duplex (Figure 1), permitting assignment of the former to terminal dG·dC base pair 1 and the latter to dG·dC base pair 2 in the sequence (Table I). This completes the assignment of the imino protons in the 12-mer GA duplex at −10 °C (Figures 2A and 3A), and their chemical shifts are listed in Table I.

Table I: A Comparison of the Imino Proton Chemical Shifts in the 12-mer and 12-mer GA Duplexes at −10 °C

	chemical shift (ppm)	
base pair	12-mer[a]	12-mer GA[b]
dG·dC 1	13.29	13.13
dG·dC 2	13.14	13.05
dG-dC 4	12.75	12.74
dA·dT 5	13.99	13.90
dA-dT 6	13.89	13.77
	chemical shift (ppm)	
	dG-dC	dG·dA
position 3	12.96	13.20

[a] Buffer: 0.1 M phosphate–H_2O, pH 7.5. [b] Buffer: 0.1 M NaCl–5 mM phosphate–H_2O, pH 6.75.

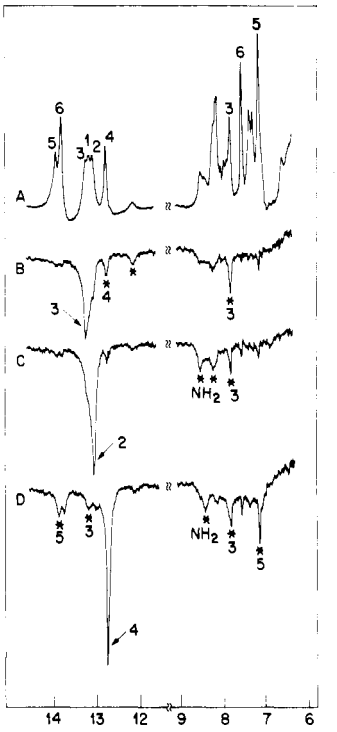

FIGURE 3: (A) The 498-MHz proton NMR spectra (11.5–14.5 ppm; 6.5–9.0 ppm) of the 12-mer GA duplex in 0.1 M NaCl, 5 mM phosphate, 1 mM EDTA, and 4:1 H_2O–D_2O, pH 6.75 at −10 °C. Difference spectra following 1-s saturation of (B) the 13.20 ppm guanosine imino proton, (C) the 13.05 ppm guanosine imino proton, and (D) the 12.74 ppm guanosine imino proton. Saturation power levels resulted in ~50% saturation of the desired resonance. The saturated resonance is designated by an arrow while the observed NOEs are designated by asterisks.

We also observe additional smaller NOEs in the difference spectra of the 12-mer GA duplex at −10 °C in Figure 3C,D. Thus, saturation of the 13.05 ppm imino proton of base pair 2 results in a small NOE at the 12.74 ppm imino proton of base-pair 4 in Figure 3C. This reflects contributions from second-order effects due to spin diffusion at this low temperature with the NOE transmitted from base pair 2 to 3 and then from 3 to 4.

NOEs between Imino and Adenosine H-2 Protons. The adenosine H-2 protons at positions 5 and 6 (dA·dT pairs) and at position 3 (dG·dA interaction) can be readily differentiated from other aromatic protons due to their long spin–lattice

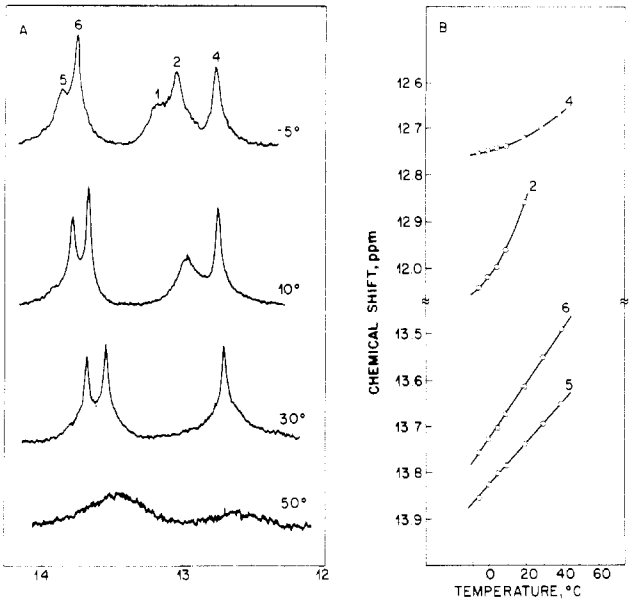

FIGURE 4: Temperature dependence of (A) the 498-MHz imino proton NMR spectra (12.5–14 ppm) and (B) the imino proton chemical shifts of the 12-mer GA duplex in 0.1 M phosphate, 1 mM EDTA, and 4:1 H_2O–D_2O, pH 7.36, between −5 and 50 °C.

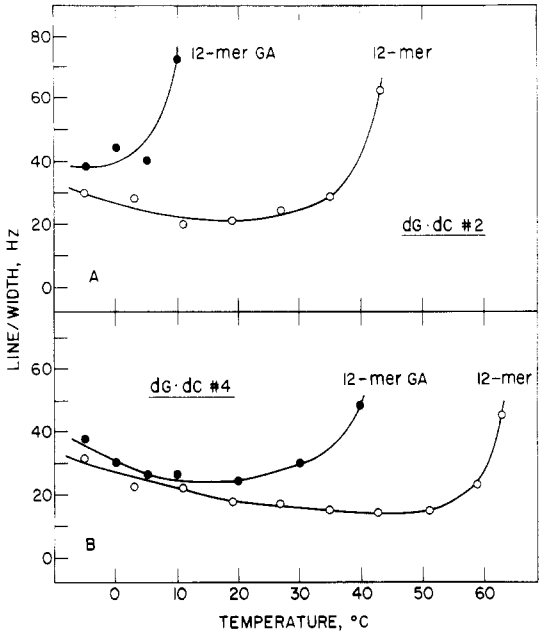

FIGURE 5: Temperature dependence of the line widths of the imino protons of (A) dG·dC base pair 2 and (B) dG·dC base pair 4 in the 12-mer (○) and 12-mer GA (●) duplexes in 0.1 M phosphate and 4:1 H_2O–D_2O. The pH values were 7.50 (12-mer) and 7.36 (12-mer GA).

relaxation times and narrow line widths and are located at 7.78, 7.51, and 7.11 ppm (Figure 2). We observe NOEs of the adenosine H-2 protons at 7.51 and 7.11 ppm on saturation of either thymidine imino proton in the difference spectra of the 12-mer GA duplex at −10 °C (Figure 2B,C). Saturation of the 13.90 ppm imino proton of dA·dT base pair 5 results in a larger NOE at the 7.11 ppm adenosine H-2 proton (Figure 2B), which must be assigned to position 5 (Table II). By contrast, saturation of the 13.77 ppm imino proton of dA·dT base pair 6 results in a larger NOE at the 7.51 ppm adenosine H-2 (Figure 2C), which must be assigned to position 6 (Table II). It should be noted that there is no NOE at the 7.78 ppm adenosine H-2 of the dG·dA interaction at position 3 on saturation of the 13.7–14.0 ppm spectral region.

Saturation of the 13.20 ppm guanosine imino proton of dG·dA interaction 3 results in an intramolecular NOE at the 7.78 ppm adenosine H-2 of the same pair (Figure 3B), requiring that these two protons be proximal to each other. We also observe NOEs at the 7.78 ppm adenosine H-2 of base pair 3 on saturation of the 13.05 ppm guanosine imino proton of adjacent base pair 2 (Figure 3C) and the 12.74 ppm guanosine imino proton of adjacent base pair 4 (Figure 3D), requiring that the adenosine H-2 proton in the dG·dA interaction be directed into the interior of the duplex and stacked over the guanosine imino protons of adjacent dG·dC base pairs.

Imino Proton Shifts in 0.1 M Phosphate. Our previous NMR studies on the 12-mer and its helix interruption and 12-mer GT mismatch analogues were investigated in 0.1 M phosphate solution (Patel et al., 1982b,c). We have therefore investigated the 12-mer GA in this buffer so that a direct comparison could be undertaken between the 12-mer and 12-mer GA duplexes. The 12-mer GA imino proton NMR spectra between −5 and 50 °C are shown in Figure 4A. The imino proton of dG·dC base-pair 1 broadens out above 0 °C, and that of dG·C base pair 2 broadens out above 20 °C, while the imino protons of base pairs 4–6 broaden simultaneously at 50 °C (Figure 4A).

The temperature dependence of the imino protons of base pairs 2 and 4–6 in the 12-mer GA in 0.1 M phosphate is plotted in Figure 4B. The thymidine imino protons of central dA·dT base pairs 5 and 6 exhibit a larger temperature coefficient than dG·dC base pair 4 over this temperature range. We also observe a large temperature coefficient at the imino proton of dG·dC base pair 2 toward the end of the duplex (Figure 4B).

Imino Proton Line Widths in 0.1 M Phosphate. The line widths of the imino protons of dG·dC base pairs 2 and 4 flanking the dG·dA mismatch site in the 12-mer GA in 0.1 M phosphate, pH 7.36 (Figure 4A), have been monitored between −5 and 50 °C and compared with the corresponding line widths for the 12-mer in 0.1 M phosphate, pH 7.50, in Figure 5. The imino protons broaden out when their exchange rates exceed 200 s^{-1}, and we note that the imino protons of dG·dC base pairs 2 and 4 broaden out at a much lower temperature in the 12-mer GA when compared with the 12-mer duplex.

Hydrogen-Exchange Kinetics. We have monitored the hydrogen exchange kinetics of the internal imino protons in the 12-mer GA duplex containing a dG·dA mismatch at position 3 and have compared them with the corresponding parameters in the 12-mer duplex with a standard dG·dC base pair at the same position. The kinetic values have been estimated from saturation recovery analysis of the resolved and assigned imino protons by measuring the recovery of magnetization as a function of the delay between the saturation and observation pulses.

The saturation-recovery lifetimes can be estimated from semilogarithmic plots of the fractional saturation as a function of the delay, and the experimental data plotted in Figure 6 yield lifetimes of 140, 198, and 244 ms for the imino protons at positions 4–6 in the 12-mer GA duplex in 0.1 M phosphate, pH 6.97, at 30 °C. These experiments have been undertaken as a function of temperature, and the saturation-recovery lifetimes between 5 and 40 °C are tabulated in Table II. The saturation-recovery lifetimes of the imino protons at positions 4–6 in the 12-mer GA duplex in 0.1 M phosphate, 30 °C, at pH 8.54 have also been measured (Table II) to estimate the effect of alkaline pH on the observed lifetimes.

Arrhenius plots of the temperature-dependent experimental saturation-recovery data for the imino protons of base pairs

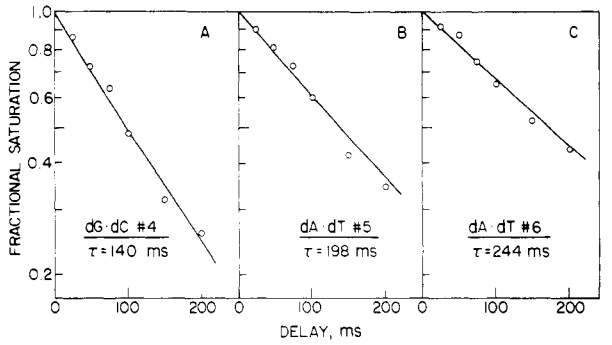

FIGURE 6: Recovery of magnetization plotted as the fractional saturation as a function of the delay between saturation and observation pulses for the imino protons (A) dG·dC base pair 4, (B) dA·dT base pair 5, and (C) dA·dT base pair 6 for the 12-mer GA duplex in 0.1 M phosphate 2.5 mM EDTA, and 4:1 H_2O–D_2O, pH 6.97, at 30 °C.

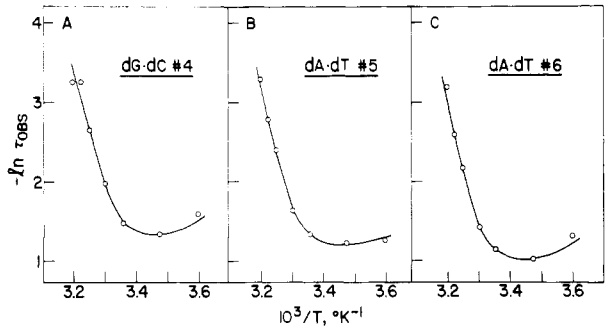

FIGURE 7: Arrhenius plots for the saturation recovery rates for the imino protons of (A) dG·dC base pair 4, (B) dA·dT base pair 5, and (C) dA·dT base pair 6 for the 12-mer GA duplex in 0.1 M phosphate, 2.5 mM EDTA, and 4:1 H_2O–D_2O, pH 6.97, between 5 and 40 °C.

Table II: Temperature and pH Dependence of the Saturation-Recovery Lifetimes of the Imino Protons in the 12-mer GA Duplex[a]

temp (°C)	imino proton lifetimes (ms) 4	5	6
	pH 6.97		
5	205	285	292
15	262	292	364
25	228	265	321
30	140	198	244
35	71	91	116
37.5	39	62	75
40	39	37	41
	pH 8.54		
30	72	108	140

[a] Buffer: 0.1 M phosphate, 2.5 mM EDTA, and 4:1 H_2O–D_2O.

4–6 in the 12-mer GA duplex in 0.1 M phosphate, pH 6.97, are shown in Figure 7. The recovery rates are essentially temperature independent below room temperature but increase dramatically on raising the temperature above ambient values (Figure 7).

Nonexchangeable Proton Spectra. The resolution-enhanced nonexchangeable proton spectra (5.2–8.2 ppm) of the 12-mer GA duplex in 0.1 M phosphate–D_2O, 25 °C, exhibit well-resolved resonances as shown in Figure 8. The resonances have been assigned to specific positions in the sequence where possible from comparisons with the known assignments in the 12-mer duplex and from one-dimensional intra and inter base pair NOEs of all the resolved base protons in the spectrum. These chemical shift values in the 12-mer GA at 25 °C are listed in Tables III and IV along with the 12-mer values for comparison.

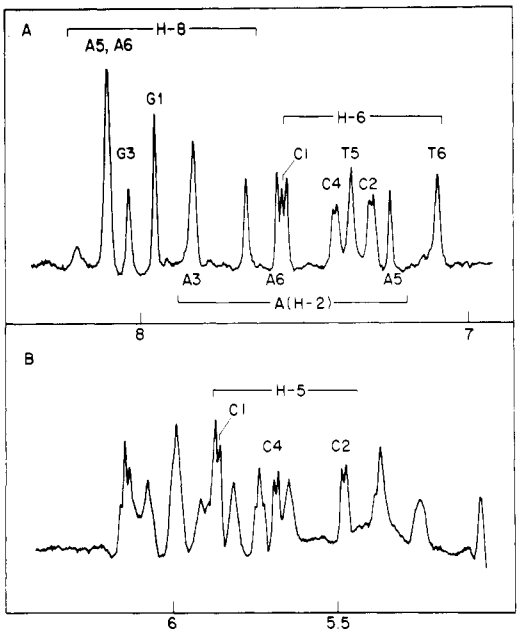

FIGURE 8: The 498-MHz proton NMR spectrum (5–8.5 ppm) of the 12-mer GA duplex in 0.1 M phosphate, 2.5 mM EDTA, and D_2O, pH 7.22, at 25 °C. The resolution of the spectrum was improved by convolution difference with line broadening of 0 and 25 Hz. The pyrimidine H-5 and H-6 and adenosine H-2 protons have been completely assigned while the purine H-8 protons are partially assigned.

Table III: A Comparison of the Nonexchangeable Proton Chemical Shifts of the 12-mer and 12-mer GA Duplexes in 0.1 M Phosphate–D_2O Solution at 25 °C

base pair	resonance	chemical shift (ppm) 12-mer	12-mer GA
dA·dT 6	$T(CH_3$-5)		
	T(H-6)	7.09	7.09
	A(H-2)	7.61	7.58
	A(H-8)	8.08	8.10
dA·dT 5	$T(CH_3$-5)	1.53	1.52
	T(H-6)	7.36	7.36
	A(H-2)	7.23	7.24
	A(H-8)	8.08	8.10
dG·dC 4	G(H-8)	7.83	*a*
	C(H-5)	5.62	5.69
	C(H-6)	7.45	7.41
dG·dC 2	G(H-8)	7.94	*a*
	C(H-5)	5.42	5.48
	C(H-6)	7.31	7.29
dG·dC 1	G(H-8)	7.94	7.95
	C(H-5)	5.91	5.87
	C(H-6)	7.62	7.56

[a] We are unable to assign the guanosine H-8 resonances at positions 2 and 4 in the 12-mer GA duplex at 25 °C at this time. The singlets at 7.68 and 7.84 ppm are potential candidates.

Table IV: Nonexchangeable Proton Chemical Shifts at Position 3 in the 12-mer and 12-mer GA Duplexes in 0.1 M Phosphate–D_2O Solution at 25 °C

resonance	chemical shift (ppm) dG·dC	dG·dA
C(H-5)	5.35	
C(H-6)	7.25	
G(H-8)	7.89	8.04
A(H-8)		*a*
A(H-2)		7.84

[a] We are unable to assign the adenosine H-8 proton at this time.

Nonexchangeable Proton NOEs. Interbase pair NOEs were previously demonstrated between the pyrimidine H-5 and

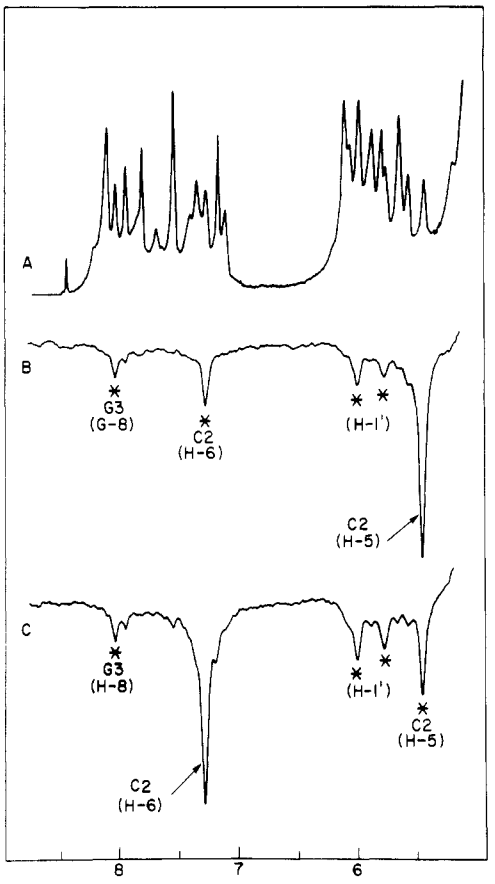

FIGURE 9: (A) The 498-MHz proton spectrum (5–9 ppm) of the 12-mer GA duplex in 0.1 M phosphate, 2.5 mM EDTA, and D_2O at 5 °C. The difference spectra following saturation of the 5.47 ppm cytidine H-5 resonance of base pair 2 and 7.29 ppm cytidine H-6 resonance of base pair 2 are shown in spectra B and C, respectively. The observed NOEs in the difference spectra are designated by asterisks. The signal to noise of spectra B and C was improved by applying a 10-Hz line-broadening contribution.

CH_3-5 protons and the H-8 proton of an adjacent purine in the 5′ direction [inter proton separation < 4 Å in the purine(3′–5′)pyrimidine step] but not in the 3′ direction [inter proton separation > 4 Å in the pyrimidine(3′–5′)purine step] in right-handed DNA (Patel et al., 1983; Feigon et al., 1983; Reid et al., 1983; Hare et al., 1983; Weiss et al., 1984). Examination of the 12-mer GA sequence (Chart II) indicates that the cytidine at position 2 is the only pyrimidine that has a purine in its 5′ direction.

The inter base pair NOE between the cytidine H-5 and H-6 protons at position 2 and the guanosine H-8 at positon 3 in the 12-mer GA at 5 °C is presented in the difference spectra in Figure 9. Saturation of either the 5.47 ppm cytidine H-5 or the 7.29 ppm cytidine H-6 protons results in an inter base pair NOE at the 8.05 ppm guanosine H-8 proton (Figures 9B,C). Thus, we are able to assign the guanosine H-8 proton at the dG·dA mismatch site to the resonance at 8.05 ppm in the 12-mer GA duplex at 5 °C.

The two remaining cytidines can be differentiated since the cytidine protons from base pair 4 exhibit inter base pair NOEs to the thymidine imino protons of adjacent base pair 5 in the 5′ direction while no such effect is observed for the cytidine protons of terminal base pair 1. The cytidine base proton chemical shifts are listed in Table III.

The thymidines at base pairs 5 and 6 can also be differentiated from each other since inter base pair NOEs are observed only between the thymidine at position 6 and the adenosine H-8 of adjacent base-pair 6 in the 5′ direction. The thymidine base proton chemical shifts are listed in Table III.

Table V: One-Dimensional NOEs (ppm) among Base Protons of the 12-mer GA Duplex in 0.1 M Phosphate–D_2O at 5 °C

	NOEs observed at			
saturate	H-8	H-6	H-5	CH_3-5
H-8				
8.12 (A5, A6)	7.83	7.13 (T6)		1.24 (T6)
8.05 (G3)		7.29 (C2)	5.46 (C2)	
H-6				
7.37 (T5)			5.68 (C4)	1.52 (T5)
				1.24 (T6)
7.29 (C2)	8.05 (G3)		5.46 (C2)	
7.13 (T6)	8.12 (A6)	7.37 (T5)		1.52 (T5)
				1.24 (T6)
H-5				
5.46 (C2)	8.05 (G3)	7.29 (C2)		
CH_3-5				
1.52 (T5)		7.13 (T6)	1.24 (T6)	
		7.37 (T5)		

We have summarized the one-dimensional NOEs on selective saturation of all the resolved base protons of the 12-mer GA duplex in Table V. NOEs are also observed at the sugar protons on saturation of the base protons, but these have not been listed in Table V.

We have also recorded selective one-dimensional NOEs in the 12-mer GA duplex at ambient temperatures (25 °C). The magnitudes of the observed NOEs are much smaller at this elevated temperature. These studies were undertaken since the singlet at 7.68 ppm is quite broad at low temperatures and we could only study NOEs involving this proton 25 °C. We observe an NOE at the 8.10 ppm adenosine H-8 proton on saturation of the 7.68 ppm resonance in the 12-mer GA at 25 °C (not shown). This suggests that the 7.68 ppm resonance is a guanosine H-8 adjacent to an adenosine H-8 on the same strand and must be assigned to the guanosine H-8 of either base pair 2 or 4.

Nonexchangeable Protons at the Mismatch Site. We have compared the chemical shifts of the three adenosine H-2 protons at positions 3, 5, and 6 for the 12-mer GA in the duplex state with the corresponding chemical shifts for the two adenosine H-2's at positions 5 and 6 for the 12-mer through the duplex to strand transition. These results are plotted in Figure 10 with the adenosine H-2s at positions 5 and 6 exhibiting similar chemical shifts for the 12-mer and 12-mer GA duplexes. The adenosine H-2 at the G·A mismatch site resonates at 7.83 ppm and is the least shielded of the three adenosines in the 12-mer GA duplex (Figure 10).

Helix–Coil Transition. We have monitored the 12-mer GA duplex to strand transition by monitoring the chemical shifts of the thymidine H-6 proton of base pair 6 and the thymidine CH_3 group of base pair 5 as a function of temperature. The melting curves for the 12-mer and 12-mer GA in 0.1 M phosphate are plotted in Figure 11, and we observe a drop in the transition midpoint from 72 °C in the parent dodecanucleotide to 55 °C on replacement of two dG·dC base pairs by two dG·dA base pairs.

Phosphodiester Backbone. The proton noise decoupled 81-MHz phosphorus NMR spectra of the 12-mer and 12-mer GA duplexes in 50 mM phosphate buffer at low temperature (17 °C) are presented in parts A and B of Figure 12 respectively. The spectral dispersion covers a 1.2 ppm range in the 12-mer GA duplex state compared to an 0.4 ppm dispersion in the strand state. We observe a phosphorus resonance at 3.48 ppm, which is downfield from the remaining resonances

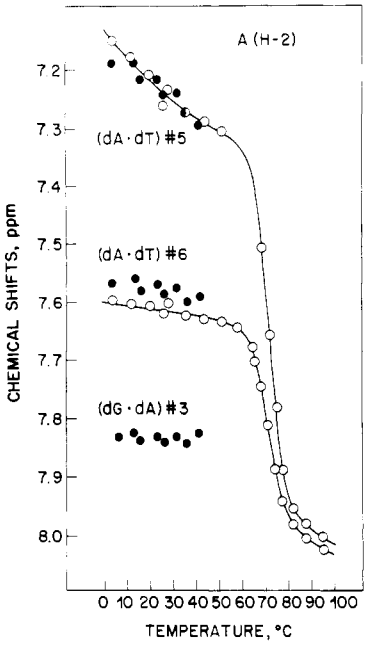

FIGURE 10: Temperature dependence of the chemical shifts of the adenosine H-2 protons at base pairs 5 and 6 in the 12-mer (O) and at base pairs 3, 5, and 6 in the 12-mer GA (●) in 0.1 M phosphate–D_2O solution.

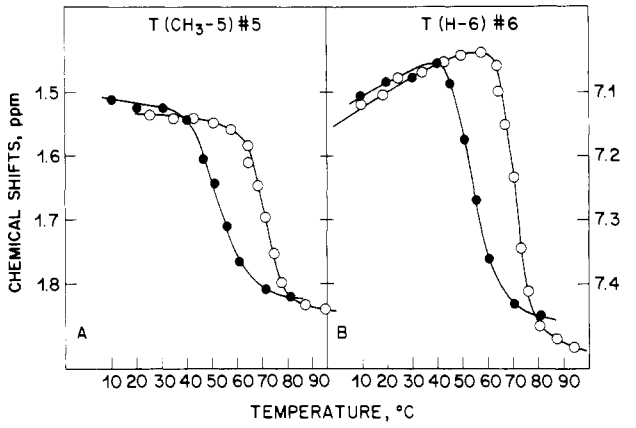

FIGURE 11: Temperature dependence of (A) base pair 5 thymidine CH_3-5 chemical shift and (B) base pair 6 thymidine H-6 chemical shift in the 12-mer (O) and 12-mer GA (●) through the melting transition in 0.1 M phosphate solution.

in the 12-mer GA duplex at 17 °C (Figure 12B). This resolved resonance characteristic of an altered phosphodiester conformation broadens and shifts into the main cluster between 35 and 55 °C (Figure 13).

Discussion

dG·dA Interaction. There are three potential dG·dA pairing modes depending on the orientation of the glycosidic bonds at the dG and dA residues. The intra base pair C1′–C1′ distance is longer than normal when both dG and dA residues are anti (Chart IIIA) but retains the regular separation for dG(anti)·dA(syn) (Chart IIIB) and dG(syn)·dA(anti,enol) (Chart IIIC) configurations. The adenosine ring is in the enol configuration for the dG(syn)·dA(anti) pairing in Chart IIIC.

Adenosine Glycosidic Angle Is Anti. The adenosine glycosidic bond is anti in Chart IIIA,C while it is syn in Chart IIIB for the dG·dA mismatch pair. We can distinguish between these two orientations of the adenosine ring since the adenosine H-2 is directed into the duplex in the anti configuration (Chart IIIA,C) while it is directed toward solvent in

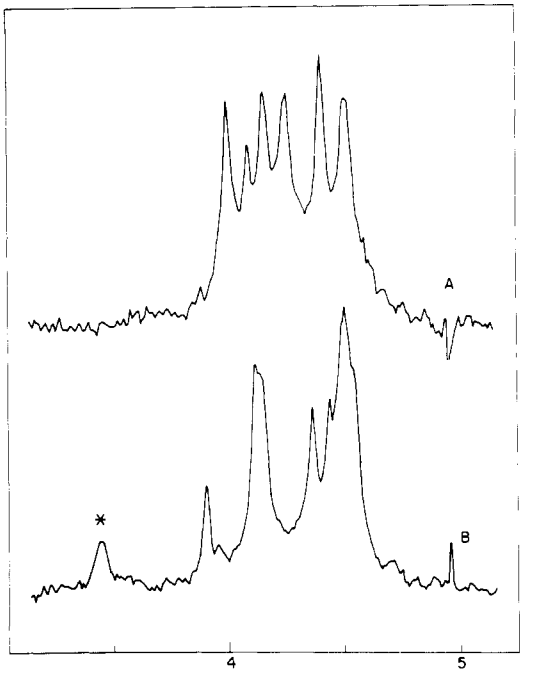

FIGURE 12: Proton noise decoupled 81-MHz phosphorus NMR spectra of (A) the 12-mer and (B) the 12-mer GA duplex in 50 mM phosphate, 1.25 mM EDTA, and D_2O at 17 °C. Chemical shifts are corrected for the temperature dependence of the internal standard trimethyl phosphate.

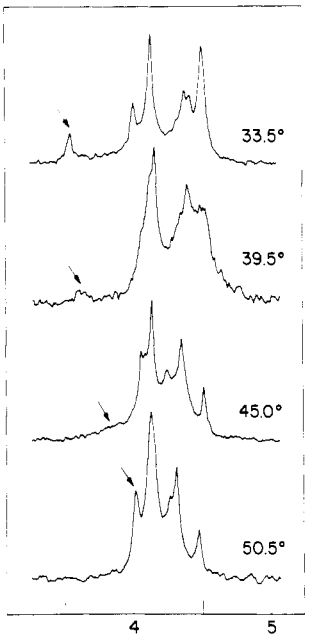

FIGURE 13: Proton noise decoupled 81-MHz phosphorus NMR spectra of the 12-mer GA in 50 mM phosphate, 1.25 mM EDTA, and D_2O as a function of temperature between 33.5 and 50.5 °C. Chemical shifts are corrected for the temperature dependence of the internal standard trimethyl phosphate.

the syn configuration (Chart IIIB). Examination of molecular models predicts NOEs between the adenosine H-2 in an anti glycosidic configuration at the dG·dA interaction and the imino protons of one or both adjacent dG·dC base pairs 2 and 4. No such NOEs are predicted for the syn configuration since the adenosine H-2 is >4 Å from the imino protons of adjacent base pairs.

Experimentally, inter base pair NOEs are observed at the 7.78 ppm adenosine H-2 on saturation of the 13.05 ppm imino protons of dG·dC base pair 2 (Figure 3C) and to a lesser extent on saturation of the 12.74 ppm imino proton of dG·dC base

Chart III

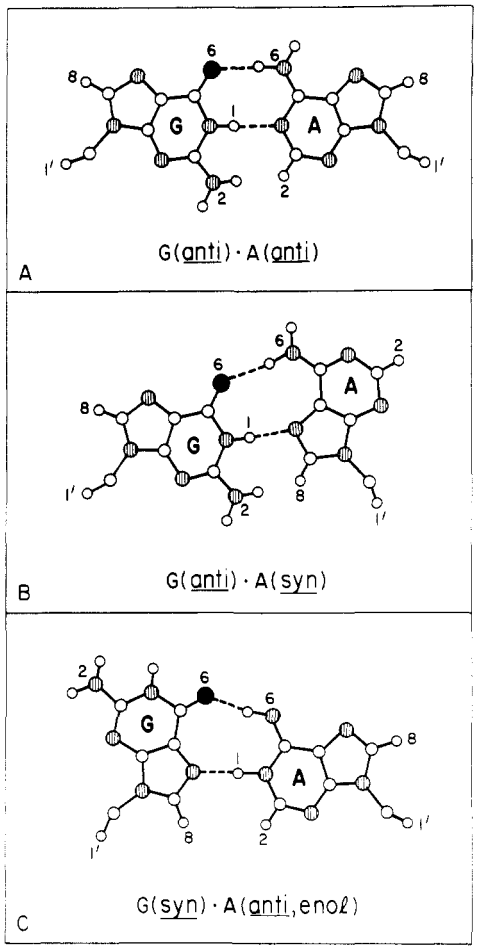

pair 4 (Figure 3D) in the 12-mer GA duplex at −10 °C. These results eliminate the dG(anti)·dA(syn) orientation (Chart IIIB) for the dG·dA interaction at position 3 in the 12 mer GA duplex.

dG(anti)·dA(anti) Pairing. The two pairing orientations in Chart IIIA,C can be differentiated from each other by monitoring intra base pair NOEs between the imino and purine nonexchangeable protons in the dG·dA interaction. Saturation of the imino proton should result in an intra base pair NOE only at the adenosine H-2 proton in Chart IIIA but at both the adenosine H-2 and guanosine H-8 protons in Chart IIIC.

Experimentally, we observe an intra base pair NOE at the 7.78 ppm adenosine H-2 proton on saturation of the 13.20 ppm imino proton in the 12-mer GA at −10 °C (Figure 3B). No NOE was observed to a narrow resonance in the guanosine H-8 spectral range centered at 7.9 ppm (Figure 3B), ruling out the orientation in Chart IIIC. Thus, the intra and inter base pair NOEs between the imino protons of guanosines at positions 2–4 and the adenosine H-2 at position 3 are consistent with the dG(anti)·dA(anti) configuration (Chart IIIA) at the dG·dA mismatch site in the 12-mer GA duplex.

Terminal and Mismatch Base Pairs. The line width of the imino exchangeable proton resonances is a measure of the stability of the base pairs relative to hydrogen exchange. The imino resonances broaden when the exchange with solvent occurs at $\geq 200\ s^{-1}$. Previous studies have demonstrated that the imino protons of terminal base pairs are most labile to exchange due to fraying at the ends of helices (Patel & Hilbers, 1975; Fritzsche et al., 1983). We note that the guanosine imino proton in the dG·dA interaction at position 3 broadens out at a somewhat lower temperature than the guanosine imino proton of terminal dG·dC base pair 1 on raising the temperature of the 12-mer GA duplex in 0.1 M NaCl–5 mM phosphate from −10 to 5 °C (Figure 1).

This result is in contrast to previous studies that established that the guanosine and thymidine imino protons in the dG·dT interaction at base pairs 3 were more kinetically stable than the guanosine imino proton of terminal dG·dC base pair 1 in the 12-mer GT duplex (Patel et al., 1982c; Pardi et al., 1982). These results establish that the imino proton in the dG·dA base pairs is much more kinetically labile than the imino protons in the dG·dT base pair when flanked by standard Watson–Crick dG·dC base pairs in an oligonucleotide duplex.

Base Pairing Adjacent to Mismatch Site. The imino protons of dG·dC base pairs 2 and 4 adjacent to the dG·dA mismatch site exhibit narrow line widths in the 12-mer GA spectrum in 0.1M NaCl–5 mM phosphate at 5 °C (Figure 1). This establishes that the base pairs are intact adjacent to the dG·dA mismatch site at low temperatures.

The imino protons of dG·dC base pairs 2 and 4 in the 12-mer GA duplex broaden out at lower temperatures (35 °C for base pair 2 and 25 °C for base pair 4) than the same imino protons in the 12-mer duplex under the same buffer conditions of ~0.1 M phosphate, pH ~7.4 (Figure 5). By contrast, the transition midpoint for the 12-mer GA is 17 °C lower than for the 12-mer in these buffer conditions (Figure 11). This establishes that dG·dC base pairs 2 and 4 are kinetically more labile as a result of incorporation of a dG·dA mismatch at adjacent base pair 3 in the sequence.

We observe a large temperature dependence of the imino proton chemical shift of dG·dC base pair 2 when compared to dG·dC base pair 4 in the 12-mer GA duplex between −5 and 40 °C (Figure 4B). By contrast, both these dG·dC imino protons exhibited a similar small premelting chemical shift in the 12-mer duplex (Patel et al., 1982b). The premelting transition may reflect changes in the extent of base-pair propeller twisting and/or base sliding with temperature (Patel et al., 1982b; Keepers et al., 1982), and the present studies establish this process for dG·dC base pair 2 adjacent to the mismatch site.

dG·dA Interactions at Low Temperature. We observe a broad exchangeable resonance at 12.11 ppm in the 12-mer GA spectrum in 0.1 M NaCl–5 mM phosphate, pH 6.75, at −10 °C (Figure 2A). This resonance broadens significantly on raising the temperature to 0 °C under these buffer conditions. We observe an NOE at the 12.11 ppm proton on saturation of the imino proton in the dG·dA pair at position 3 (Figure 3B) but not on saturation of the imino protons of dA·dT base pairs 5 (Figure 2B) and 6 (Figure 2C).

These results suggest that there may be two conformations of the dG·dA mismatch in slow exchange at low temperatures with the predominant dG(anti)·dA(anti) base-paired form (Chart IIIA) represented by the 13.20 ppm imino proton while the minor form is represented by the 12.11 ppm resonance. We are unable to decipher structural information on the dG·dA pairing in the minor form.

dA·dT Core of the Duplex. The dA·dT imino proton spectral region exhibits an asymmetric pattern in the 12-mer GA duplex at low temperature (Figures 1 and 4) with the resonance from base pair 5 somewhat broader and less intense than that from base pair 6. This asymmetry was not observed for the imino protons in the 12-mer (Patel et al., 1982b) and 12-mer GT duplexes (Patel et al., 1982c). This difference becomes less pronounced in the 12-mer GA duplex on raising the temperature with the imino resonances from dG·dC base pair 4 and dA·dT base pairs 5 and 6 broadening out simultaneously above 50 °C (Figure 4A).

This low-temperature asymmetry may arise from the imino proton of dA·dT base pair 5 exhibiting a chemical shift at 13.90 ppm for the predominant dG·dA mismatch conformation and a chemical shift at 13.77 superpositioned on the imino proton of dA·dT base pair 6 for the minor conformation of the mismatch. This may explain why an NOE is observed at the 12.74 ppm imino proton of dG·dC base pair 4 when either the 13.90 (Figure 2A) or 13.77 ppm (Figure 2B) resonance is saturated in the 12-mer GA duplex at −10 °C, but this NOE is much attenuated when the latter is saturated at 5 °C.

The chemical shifts of both dA·dT imino protons in the 12-mer GA duplex exhibit large slopes between −5 and 40 °C (Figure 4B), establishing a premelting transition in the central core of the 12-mer GA duplex similar to what has been observed previously in the 12-mer duplex (Patel et al., 1982b).

Stacking of Adenosine Bases. The adenosine H-2 protons of base pairs 5 and 6 in the 12-mer GA duplex exhibit similar chemical shifts to the 12-mer duplex in the premelting transition region (Figure 10). These observations suggest that the stacking of adenosine rings at positions 5 and 6 in the d(A-A-T-T) center of the duplex is not perturbed by the introduction of dG·dA mismatches at position 3 in either direction.

The adenosine H-2 proton of the dG·dA mismatch at position 3 resonates at 7.78 ppm in the 12-mer GA duplex between 0 and 40 °C (Figure 10). This chemical shift is upfield from its unstacked strand value of 8.2 ppm at high temperature and reflects shielding contributions from the ring currents of adjacent stacked base pairs. Such an upfield shift is consistent with an anti glycosidic torsion angle where the adenosine H-2 is directed into the duplex.

Chemical Shifts about the Mismatch Site. We have compared the base proton chemical shifts of the 12-mer and 12-mer GA duplexes at the imino protons (Table I), the nonexchangeable protons of standard Watson–Crick pairs (Table III), and the dG·dA mismatch pair (Table IV). There are no major perturbations in chemical shifts (>0.1 ppm) for the majority of the base protons at positions 2 and 4 on replacing the dG·dC base pair by a dG·dA interaction at position 3 (Tables I and III). We do note, however, that the guanosine H-8 for base pairs flanking position 3 resonates at 7.83 and 7.94 ppm in the 12-mer compared to applied values of 7.68 and 7.84 ppm in the 12-mer GA duplex (Table III). The lack of chemical shift changes between the 12-mer and the 12-mer GA is somewhat surprising since we are replacing a pyrimidine by a purine ring to generate a dG·dA interaction.

Both the guanosine imino and H-8 protons in the dG·dA mismatch resonate to low field of their values in the dG·dC pair at position 3 (Tables I and IV), most likely due to the larger in plane ring current deshielding of the adenosine ring. The imino proton of the dG·dA mismatch in the 12-mer GA duplex resonates at 13.20 ppm (Table I), which is in the chemical shift range (12.6–13.6 ppm) for the imino protons of standard dG·dC pairs.

The 13.20 ppm chemical shift of the imino proton in the dG(anti)·dA(anti) mismatch of the 12-mer GA duplex is consistent with a NH···N hydrogen-bonding interaction as depicted in Chart IIIA. This contrasts with proton chemical shifts of 11.78 and 10.58 ppm for the imino protons in the dG·dT wobble pair with NH···O hydrogen-bonding interactions (Patel et al., 1982c).

Transition Midpoint. We previously demonstrated that replacement of the dG·dC base pairs at position 3 in the 12-mer duplex by dG·dT base pairs in the 12-mer GT duplex resulted in a decrease in the transition midpoint from 72 to ~52 °C in 0.1 M phosphate solution. The present studies demonstrate that replacement with two dG·dA base pairs in the 12-mer GA duplex results in a decrease in the transition midpoint to ~55 °C in 0.1 M phosphate as monitored by the thymidine proton markers at central positions 5 and 6 (Figure 11). Thus, we observe similar destabilization of a dodecanucleotide duplex on replacement of internal dG·dC base pairs by either the dG·dT purine–pyrimidine mismatch (Patel et al., 1982c) or the dG·dA purine–purine mismatch.

Scheme I

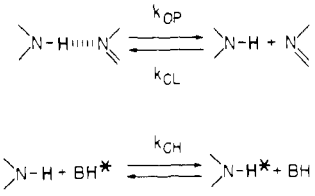

Hydrogen-Exchange Pathways. Previous studies on transfer RNA (Johnston & Redfield, 1977, 1981; Hurd & Reid, 1980) and DNA (Early et al., 1981a,b; Pardi & Tinoco, 1982; Pardi et al., 1982, 1983; Patel et al., 1983b) oligonucleotides have established that the magnetic contribution to the saturation-recovery rates predominates at low temperature while the hydrogen-exchange contribution predominates above room temperature. Our interest is directed toward the hydrogen-exchange parameters, and hence, we focus on the saturation-recovery lifetimes for the 12-mer GA between 25 and 45 °C (Table II and Figure 7).

Exchange can occur from the transiently open form as outlined in the general scheme for hydrogen exchange in Scheme I. The exchange pathway is dependent on the relative magnitudes of k_{CL} and $k_{CH}[BH]$ (Teitelbaum & Englaender, 1975a,b).

For the case where $k_{CL} \gg k_{CH}[BH]$, the paired and open states are in rapid equilibrium with occasional leakage from the open state with solvent H_2O. The hydrogen-exchange rate is given by

$$k_{EX} = \frac{k_{OP}}{k_{CL}} k_{CH}[BH]$$

and is directly dependent on the concentration of base or general buffer catalyst. Earlier studies demonstrated that this pathway predominates for base pairs that fray at the ends of DNA duplexes (Patel & Hilbers, 1975).

For the case where $k_{CH}[BH] \gg k_{CL}$, exchange occurs every time the base pair transiently opens, and the hydrogen-exchange rate is given by

$$k_{EX} = k_{OP}$$

The exchange rate is a direct measure of the base pair opening rate and is independent of base and general buffer catalyst.

We have measured the imino proton lifetimes of dG·dC base pair 4 and dA·dT base pairs 5 and 6 in the 12-mer GA in 0.1 M phosphate at pH 6.97 and 8.54 at 30 °C (Table II). The exchange lifetimes are approximately a factor of 2 shorter at positions 4–6 on raising the base concentration by a factor of ~15. This result suggests that the helix opening and, to a smaller extent, the preequilibrium pathways both contribute to the 12-mer GA exchange mechanism at 30 °C. By contrast, the helix-opening pathway contributed solely to hydrogen exchange at base pairs 4–6 in the 12-mer and 12-mer GT duplexes reported previously (Pardi et al., 1982).

Kinetic Destabilization Adjacent to Mismatch Site. We have compared the saturation-recovery lifetimes at dG·dC base pair 4 and dA·dT base pairs 5 and 6 in the 12-mer and 12-mer GA duplexes in 0.1 M phosphate, pH 7, at 30 °C (Table VI).

Table VI: A Comparison of the Imino Proton Lifetimes (30 °C) and the Saturation-Recovery Activation Barriers for the 12-mer (pH 6.95) and the 12-mer GA (pH 6.97) Duplexes in 0.1 M Phosphate, 2.5 mM EDTA, and 4:1 H_2O–D_2O Solution

	imino proton lifetimes (ms) at 30 °C		
	4	5	6
12-mer	358	184	310
12-mer GA	140	198	244
	saturation-recovery barriers (kcal)[a]		
	4	5	6
12-mer		17	17.5
12-mer GA	29	32	35

[a] The activation barriers were directly computed from the slope of the saturation-recovery data between 30 and 40 °C (Figure 7).

We observe a kinetic destabilization of a factor of 2.5 at dG·dC base pair 4 on replacing a standard dG·dC base pair by a dG·dA pair at adjacent position 3 in the dodecanucleotide duplex. This destabilization is a localized effect since it does not extend to dA·dT base pair 5, which is one removed from the mismatch site (Table VI). A similar localized perturbation was observed on comparison of the saturation-recovery parameters of the 12-mer and 12-mer GT duplexes (Pardi et al., 1982).

Activation Barriers for Hydrogen Exchange. The activation barriers have been directly computed from the slope of the saturation-recovery data between 30 and 40 °C at positions 4–6 in the 12-mer GA duplex in 0.1 M phosphate (Figure 7). The activation energies for the saturation-recovery process at dA·dT pairs 5 and 6 are approximately a factor of 2 larger in the 12-mer GA when compared to the 17-kcal barriers observed at these positions in the 12-mer (Table VI). The larger kinetic barrier for imino proton exchange in 12-mer GA demonstrates that exchange occurs by the cooperative opening of several base pairs as was previously demonstrated for the 12-mer GT duplex (Pardi et al., 1982).

Altered Phosphodiester Backbone. There are significant differences in the phosphorus spectra of the 12-mer and 12-mer GA duplexes at 17 °C (Figure 12), indicative of an altered phosphodiester backbone (Gorenstein, 1981; Patel et al., 1979) in the mismatch analogue. There is a decrease in intensity in the resonance centered about 4.2 ppm and an increase in intensity in the resonances centered about 4.5 ppm on proceeding from the 12-mer (Figure 12A) to the 12-mer GA duplex (Figure 12B).

The 3.48 ppm resonance in the 12-mer GA duplex at 17 °C resonates outside the normal 4.5–5.0 ppm region observed in duplexes containing standard dA·dT and dG·dC base pairs only (Figure 12B). The resolved resonance at 3.48 ppm broadens and shifts into the 4.0–4.5 ppm cluster on raising the temperature of the 12-mer GA to 50 °C in 50 mM phosphate solution (Figure 13). This transition occurs at a lower temperature (~42 °C) compared to the melting transition of 55 °C monitored by the nonexchangeable protons for the 12-mer GA in 100 mM phosphate solution (Figure 11).

Molecular Mechanics Calculations. J. W. Keepers, P. Schmidt, and P. A. Kollman (unpublished results) have undertaken molecular mechanics calculations on the 12-mer GA duplex. They can readily incorporate a dG(anti)·dA(anti) interaction into the DNA helix and have estimated the destabilization resulting from replacement of two dG·dC base pairs by two dG·dA pairs (J. W. Keepers, P. Schmidt, and P. A. Kollman (unpublished results). Conformational details of potential low-energy conformations for the 12-mer GA duplex are summarized (J. W. Keepers, P. Schmidt, and P. A. Kollman, unpublished results).

General Conclusions. We wish to bring attention to a preliminary NMR study on dG·dA mismatches located adjacent to each other in the d(C-C-A-A-G-A-T-T-G-G) decanucleotide duplex published recently (Kan et al., 1983). These authors have used one-dimensional NOEs to conclude that both dG and dA are in the anti configuration for the dG·dA mismatches that are adjacent to each other in this duplex (Kan et al., 1983). There is thus good agreement between the investigation of Kan et al. (1983) and our studies on dG·dA mismatches separated by six base pairs in the 12-mer GA duplex.

Acknowledgments

We acknowledge helpful discussions with Dr. Horace Drew on potential pairing modes for the dG·dA mismatch pair.

References

Arnott, S. Chandrasekaran, R., Hall, I. H., Puigjaner, L. C., Walker, J. K., & Wang, M. (1983) *Cold Spring Harbor Symp. Quant. Biol. 47*, 53–65.

Dickerson, R. E., Drew, H. R., Conner, B. N., Wing, R. M., Fratini, A. V., & Kopka, M. L. (1982) *Science (Washington, D.C.) 216*, 475–485.

Dickerson, R. E., Drew, H. R., Conner, B. N., Kopka, M. L., & Pjura, P. E. (1983) *Cold Spring Harbor Symp. Quant. Biol. 47*, 13–24.

Dodgson, J. B., & Wells, R. D. (1977a) *Biochemistry 16*, 2367–2374.

Dodgson, J. B., & Wells, R. D. (1977b) *Biochemistry 16*, 2374–2379.

Early, T. A., Olmsted, J., III, Kearns, D. R., & Lexius, A. G. (1978) *Nucleic Acids Res. 5*, 1955–1970.

Early, T. A., Kearns, D. R., Hillen, W., & Wells, R. D. (1980) *Nucleic Acids Res. 8*, 5795–5812.

Early, T. A., Kearns, D. R., Hillen, W., & Wells, R. D. (1981a) *Biochemistry 20*, 3756–3764.

Early, T. A., Kearns, D. R., Hillen, W., & Wells, R. D. (1981b) *Biochemistry 20*, 3764–3769.

Feigon, J., Wright, J. M., Denny, W. A., Leupin, W., & Kearns, D. R. (1983) *Cold Spring Harbor Symp. Quant. Biol. 47*, 207–217.

Fritzsche, H., Kan, L. S., & Tso, P. O. P. (1983) *Biochemistry 22*, 277–280.

Gorenstein, D. G. (1981) *Annu. Rev. Biophys. Bioeng. 10*, 355–386.

Haasnoot, C. A. G., den Hartog, J. H. J., de Rooij, J. F., van Boom, J. H., & Altona, C. (1979) *Nature (London) 281*, 235–236.

Haasnoot, C. A. G., den Hartog, J. H. J., de Rooij, J. F., van Boom, J. H., & Altona, C. (1980) *Nucleic Acids Res. 8*, 169–181.

Hare, D. R., & Reid, B. R. (1982) *Biochemistry 21*, 1835–1842.

Hare, D. R., Wemmer, D. E., Chou, S. H., Drobny, G., & Reid, B. R. (1983) *J. Mol. Biol. 171*, 319–336.

Hurd, R. E., & Reid, B. R. (1980) *J. Mol. Biol. 142*, 181–193.

Johnston, P. D., & Redfield, A. G. (1977) *Nucleic Acids Res. 4*, 3599–3615.

Johnston, P. D., & Redfield, A. G. (1981) *Biochemistry 20*, 3996–4006.

Kan, L. S., Cheng, D. M., Jayaraman, K., Lentzinger, E. E., Miller, P. S., & T'so, P. O. P. (1982) *Biochemistry 21*, 6723–6732.

Kan, L., Chandrasekaran, S., Pulford, S. M., & Miller, P. S. (1983) *Proc. Natl. Acad. Sci. U.S.A. 80*, 4263–4265.

Kaptein, R., Scheek, R. M., Zuiderweg, E. R. P., Boelens, R., Klappe, K. J. M., van Boom, J. H., Ruterjans, H., & Beyrenther, K. (1983) in *Structure and Dynamics: Nucleic Acids and Proteins* (Clementi, E., & Sarma, R. H., Eds.) pp 209–225, Adenine Press, New York.

Keepers, J. W., Kollman, P. A., Weiner, P. K., & James, T. L. (1982) *Proc. Natl. Acad. Sci. U.S.A. 71*, 5537–5541.

Kim, S. H. (1981) in *Topics in Nucleic Acid Structure* (Neidle, S., Ed.) pp 83–112, Halsted Press, London.

Levitt, M. (1983) *Cold Spring Harbor Symp. Quant. Biol. 47*, 251–262.

Lomant, A. J., & Fresco, J. R. (1975) *Prog. Nucleic Acid Res. Mol. Biol. 15*, 185–218.

Neidle, S., & Berman, H. M. (1983) *Prog. Biophys. Mol. Biol. 41*, 43–66.

Olson, W. K. (1982) *Top. Nucleic Acid Struct. 2*, 1–80.

Olson, W. K., Srinivasan, A. R., Marky, N. L., & Balaji, V. N. (1983) *Cold Spring Harbor Symp. Quant. Biol. 47*, 229–241.

Pardi, A., & Tinoco, I., Jr. (1982) *Biochemistry 21*, 4686–4693.

Pardi, A., Martin, F. H., & Tinoco, I., Jr. (1981) *Biochemistry 20*, 3986–3996.

Pardi, A., Morden, K. M., Patel, D. J., & Tinoco, I., Jr. (1982) *Biochemistry 21*, 6567–6574.

Pardi, A., Morden, K. M., Patel, D. J., & Tinoco, I., Jr. (1983) *Biochemistry 22*, 1107–1113.

Patel, D. J., & Hilbers, C. W. (1975) *Biochemistry 14*, 2651–2656.

Patel, D. J., Canuel, L. L., & Pohl, F. M. (1979) *Proc. Natl. Acad. Sci. U.S.A. 76*, 2508–2511.

Patel, D. J., Pardi, A., & Itakura, K. (1982a) *Science (Washington D.C.) 216*, 581–590.

Patel, D. J., Kozlowski, S. A., Marky, L. A., Broka, C., Rice, J. A., Itakura, K., & Breslauer, K. J. (1982b) *Biochemistry 21*, 428–436.

Patel, D. J., Kozlowski, S. A., Marky, L. A., Rice, J. A., Broka, C., Dallas, J., Itakura, K., & Breslauer, K. (1982c) *Biochemistry 21*, 437–444.

Patel, D. J., Kozlowski, S. A., Rice, J. A., Marky, L. A., Breslauer, K. J., Broka, C., & Itakura, K. (1982d) *Top. Nucleic Acid Struct. 2*, 81–136.

Patel, D. J., Kozlowski, S. A., Ikuta, S., Itakura, K., Bhatt, R., & Hare, D. R. (1983a) *Cold Spring Harbor Symp. Quant. Biol. 47*, 197–206.

Patel, D. J., Ikuta, S., Kozlowski, S., & Itakura, K. (1983b) *Proc. Natl. Acad. Sci. U.S.A. 80*, 2184–2188.

Redfield, A. G., Roy, S., Sanchez, V., Tropp, J., & Figueroa, N. (1981) in *Second SUNYA Conference on Biomolecular Stereodynamics* (Sarma, R. H., Ed.) pp 195–208, Adenine Press, New York.

Reid, D. G., Salisbury, S. A., Bellard, S., Shakked, Z., & Williams, D. H. (1983) *Biochemistry 22*, 2019–2025.

Rein, R., Shibata, M., Garduno-Juarez, R., & Kieber-Emmons, T. (1983) in *Structure and Dynamics: Nucleic Acids and Proteins* (Clementi, E., & Sarma, R. H., Eds.) pp 296–288, Adenine Press, New York.

Schimmel, P. R., & Redfield, A. G. (1980) *Annu. Rev. Biophys. Bioeng. 9*, 181–221.

Tan, Z. K., Ikuta, S., Huang, T., Dugaiczyk, A., & Itakura, K. (1983) *Cold Spring Harbor Symp. Quant. Biol. 47*, 383–391.

Teitelbaum, H., & Englaender, S. W. (1975a) *J. Mol. Biol. 92*, 57–78.

Teitelbaum, H., & Englaender, S. W. (1975b) *J. Mol. Biol. 92*, 79–92.

Tidor, B., Irikura, K. K., Brooks, B. R., & Karplus, M. (1983) *J. Biomol. Struct. Dyn. 1*, 231–252.

Tilton, R. F., Jr., Weiner, P. K., & Kollman, P. A. (1983) *Biopolymers 22*, 969–1002.

Topal, M. D., & Fresco, J. R. (1976a) *Nature (London) 263*, 285–289.

Topal, M. D., & Fresco, J. R. (1976b) *Nature (London) 263*, 289–295.

Traub, W., & Sussman, J. L. (1982) *Nucleic Acids Res. 10*, 2701–2708.

Viswamitra, M. A. (1983) *Cold Spring Harbor Symp. Quant. Biol. 47*, 25–31.

Wallace, R. B., Shaffer, J., Murphy, R. F., Bonner, J., Hirose, T., & Itakura, K. (1979) *Nucleic Acids Res. 6*, 3543–3557.

Wang, A. H. J., Fujii, S., van Boom, J. H., & Rich, A. (1983) *Cold Spring Harbor Symp. Quant. Biol. 47*, 33–44.

Weiss, M., Patel, D. J., Sauer, R. T., & Karplus, M. (1984) *Proc. Natl. Acad. Sci. U.S.A. 81*, 130–134.

Zimmerman, S. B., & Pheiffer, B. H. (1983) *Cold Spring Harbor Symp. Quant. Biol. 47*, 67–76.